MULTI-GNSS PPP: AN ALTERNATIVE POSITIONING TECHNIQUE FOR ESTABLISHING GROUND CONTROL POINTS

B. Bahadur [a], M. Nohutcu [a]

[a] Hacettepe University, Dept. of Geomatics Engineering, 06800 Çankaya Ankara, Turkey – berkaybahadur @hacettepe.edu.tr, mnohutcu@hacettepe.edu.tr

KEY WORDS: Ground Control Points (GCPs), GNSS, Multi-GNSS, Precise Point Positioning (PPP)

ABSTRACT:

Traditionally, ground control points (GCPs) are utilized to determine absolute image orientations indirectly in aerial triangulation. For a long time, differential and relative GNSS (Global Navigation Satellite System) positioning techniques have been extensively used to establish GCPs. In our country, the establishment and measurement of GCPs are instructed in the related regulation based on differential GNSS techniques. One of the two methods described in the related regulation is based on establishing, at least, C3 level networks with maximum base length of 10 km and with minimum 35-minute observation time. In an alternative method, without base length restriction, GCP coordinates can be determined being connected to at least 3 TUSAGA-Active stations and with minimum 120-minute static observation. The expected precision for the coordinates of GCPs are described to be better than 5 cm in horizontal and 6 cm in vertical within the regulation. Although differential techniques can provide highly accurate positioning solutions, they are required at least two receivers to mitigate GNSS error sources. Additionally, positioning accuracy obtained from these techniques are strictly dependent on the distance from reference stations. It is clear that all these raise the operational cost and system complexity of differential GNSS techniques. In recent years, Precise Point Positioning (PPP), which enables centimeter- or millimeter-level positioning accuracy with only one receiver on a global scale, has emerged as an alternative positioning method. Over the last decade, PPP has attracted considerable attention within the GNSS community due to its exceptional benefits such as operational simplicity, cost-effectiveness, elimination of base station requirement. However, the main drawback of PPP is relatively long observation period required to achieve a specific positioning accuracy, for example, nearly 50 min to reach 10 cm or better horizontal accuracy with 30 seconds sampling rate. On the other hand, the completion of GLONASS constellation and the emergence of new satellite systems, such as Galileo and BeiDou, offers considerable opportunities to improve the PPP performance. The combinations of different GNSS constellations, namely multi-GNSS, strength the number and geometry of visible satellites, and therefore, reduces the convergence time significantly. Additionally, the new generation GNSS receivers make possible to collect more observations (even up to 100Hz), which provides abundant data for PPP processing. Taking all these into account, the principal objective of this study is to investigate the usability of PPP in establishing GCPs for aerial triangulation. For this purpose, an experimental test was conducted to evaluate the positioning performance of multi-GNSS PPP with high-frequency GNSS receivers (1 Hz). The results indicate that 5 cm or better horizontal and vertical positioning accuracy can be achieved by multi-GNSS PPP process within approximately 30 minutes using high-frequency GNSS receivers. Considering these results and its operational simplicity, it can be said that PPP is a robust alternative for the establishment of GCPs.

ÇOKLU-GNSS PPP: YER KONTROL NOKTALARININ TESİSİ İÇİN ALTERNATİF POZİSYON BELİRLEME YÖNTEMİ

B. Bahadur [a], M. Nohutcu [a]

[a] Hacettepe Universitesi, Geomatik Mühendisliği Bölümü, 06800 Çankaya Ankara, Türkiye – berkaybahadur @hacettepe.edu.tr, mnohutcu@hacettepe.edu.tr

ANAHTAR KELİMELER: Yer Kontrol Noktası (YKN), GNSS, Çoklu-GNSS, Hassas Nokta Konumlama (PPP)

ÖZ:

Geleneksel olarak, yer kontrol noktaları (YKN) havai (fotogrametrik) nirengi işleminde mutlak yöneltme parametrelerinin dolaylı olarak belirlenmesi için kullanılır. Rölatif ve diferansiyel GNSS (Küresel Navigasyon Uydu Sistemi) konum belirleme teknikleri uzun yıllardır YKN'lerin tesis edilmesi için yaygın olarak kullanılmaktadır. Ülkemizde, YKN'lerin tesisi ve ölçümü için izlenecek talimatlar bu tekniklere bağlı olarak ilgili yönetmelikte belirtilmiştir. İlgili yönetmelikte tarif edilen yöntemlerden ilki, YKN'lerin baz uzunluğu en fazla 10 km olan ve ilgili noktada en az 35 dakika kayıt süresi gerektiren en az C3 derece ağ olarak tesis edilmesini temel almaktadır. Diğer alternatif yöntemde, YKN koordinatları en az 3 TUSAGA-Aktif istasyonu kullanılarak ve en az 120 dakika statik ölçü gerçekleştirerek baz uzunluğuna bağlı olmaksızın belirlenebilir. Bu yönetmelik çerçevesinde YKN koordinatlarının belirlenmesinde yatayda 5 cm düşeyde ise 6 cm hassasiyet beklenmektedir. Diferansiyel teknikler yüksek doğrulukta konumsal çözümler üretebilmesine rağmen, GNSS hata kaynaklarını ortadan kaldırmak için en az 2 adet GNSS alıcısına ihtiyaç duymaktadır. Ek olarak, bu tekniklerden elde edilecek konum doğruluğu referans istasyonlardan olan mesafeye oldukça bağlıdır. Tüm bunların diferansiyel tekniklerin işletim maliyetini ve sistem karmaşıklığını arttırdığı açıktır. Son yıllarda, bu tekniklere bir alternatif olarak, yalnızca tek bir alıcı ile global ölçekte santimetre ya da milimetre seviyesinde konum doğruluğu üretebilen Hassas Nokta Konumlama (PPP) tekniği ortaya çıkmıştır. Son on yılda, uygulama kolaylığı, düşük maliyeti ve referans istasyon ihtiyacını ortadan kaldırması gibi faydalarından dolayı PPP GNSS kullanıcıları arasında ilgi çekici bir konu olmuştur. Yine de belirli bir konum doğruluğuna ulaşabilmek için ihtiyaç duyduğu göreli uzun yakınsama süresi, örneğin 10 cm ve daha iyi yatay konum doğruluğu için 30 saniye gözlem aralığında yaklaşık 50 dakika, PPP tekniğinin en büyük dezavantajıdır. Öte yandan, GLONASS uydu takımının tamamlanması ve Galileo ve BeiDou gibi yeni navigasyon sistemlerinin ortaya çıkması PPP performansının iyileştirilmesi açısından önemli fırsatlar sunmaktadır. Birden fazla navigasyon sisteminin ortak olarak kullanılması, yani çoklu-GNSS, görünür uydu sayısı ve geometrisini iyileştirmekte ve bu sayede yakınsama süresini kısaltmaktadır. Ayrıca, yeni nesil GNSS alıcıları daha fazla gözlem (100 Hz'e kadar) toplayabilmektedir ve bu durum PPP işlemi için ilave veri anlamına gelir. Tüm bunlar göz önünde bulundurulduğunda, bu çalışmanın temel amacı PPP tekniğinin havai nirengi işleminde YKN'lerin tesisi için kullanılabilirliğinin araştırılmasıdır. Bu amaçla, yüksek-frekanslı GNSS alıcısı (1 Hz) ile çoklu-GNSS PPP performansının değerlendirilmesi için deneysel bir test gerçekleştirilmiştir. Sonuçlar, yüksek-frekanslı GNSS alıcısı kullanılarak çoklu-GNSS PPP işleminde yaklaşık 30 dakika içerisinde 5 cm ve daha iyi hem yatay hem de düşey konum doğruluğuna erişildiğini göstermektedir. Bu sonuçlar ve işlem kolaylığı göz önünde bulundurulduğunda, PPP tekniğinin YKN'lerin tesisi için güçlü bir alternatif olduğu söylenebilir.

1. INTRODUCTION

Nowadays, photogrammetric products, e.g. digital elevation models, dense point clouds and orthomosaics, are routinely produced with the imagery acquired from manned or unmanned aerial platforms (Peppa et al., 2016; Murtiyoso and Grussenmeyer, 2017). Thanks to GPS-supported aerial triangulation, the exterior orientation parameters of aerial images can be estimated with ease, which reduces the number of ground control points (GCPs) (Ackermann, 1994). However, a small number of GCPs is still required to determine absolute image orientations indirectly in aerial triangulation. In aerial photogrammetry, at least four points, one located in each corner of the image block, are typically employed to prevent systematic error in GPS camera positions (Yuan, 2009).

For a long time, differential and relative GNSS (Global Navigation Satellite System) positioning techniques have been extensively used to establish GCPs. In Turkey, instructions on how to establish and measure the GCPs are provided in the related regulation (*6961 Büyük Ölçekli Harita ve Harita Bilgileri Üretim Yönetmeliği*). Accordingly, two different methods which are based on differential GNSS techniques can be used for establishing GCPs. The first method is to employ at least C3 level networks with a maximum base length of 10 km and with minimum 35-minute observation time. Alternatively, the GCP coordinate can be determined being connected to at least 3 TUSAGA-Active stations without base-length restriction. However, minimum 120-minute static observation is required for the second method. Finally, the expected precision for these methods that are utilized in establishing GCPs are introduced to be better than 5 cm in horizontal and 6 cm in vertical within the regulation.

Differential and/or relative GNSS techniques are able to provide high-accuracy positioning solutions using reference points with known coordinates to eliminate most of GNSS observation errors. By definition, these techniques require at least two receivers (one reference and one rover) to achieve high positioning accuracy. There is no doubt that it raises the operational cost and system complexity. Moreover, the positioning accuracy of differential GNSS techniques is closely dependent on the distance from the reference station or regional network, which means that the relative or differential techniques can efficiently work in a limited area (Rizos et al., 2012).

In recent years, Precise Point Positioning (PPP) has emerged as an alternative precise positioning method to differential and/or relative techniques. PPP enables centimetre- or millimetre-level positioning accuracy with only one receiver on a global scale using the precise orbit and clock products obtained from a global network (Zumberge et al., 1997; Kouba and Héroux, 2001). PPP has taken considerable interest within the GNSS community due to its exceptional benefits such as operational simplicity, cost-effectiveness, elimination of base station requirement. However, PPP still suffers from the long initial time, namely convergence time, to achieve a specific positioning accuracy. In general, ten centimetres or better horizontal accuracy can be reached after a 50-minute observation period in the standard PPP solution (Choy, 2017).

The completion of GLONASS constellation and the emergence of new satellite systems, such as Galileo and BeiDou have offered significant opportunity to enhance the PPP positioning performance due to providing additional satellite source and new navigation signals. The combinations of different GNSS constellations, namely multi-GNSS, strength the number and geometry of visible satellites, and therefore, reduces the convergence time (Cai et al., 2015; Tegedor et al., 2014; Bahadur and Nohutcu, 2018). On the other hand, the use of high-rate (1 Hz or more frequent) observations recorded by new-generation GNSS receivers provides a possibility to improve the PPP performance thanks to increasing the number of observations substantially (Xu et al., 2013). Taking all these into account, the main objective of this study is to investigate the usability of PPP in establishing GCPs for aerial triangulation. In this context, the experimental text conducted to assess the positioning performance of multi-GNSS PPP with high-frequency GNSS receivers (1 Hz) and its results are provided in this study.

2. METHOD

This section provides a brief introduction to multi-GNSS PPP model and to PPP processing strategies applied in this model to mitigate GNSS error sources.

2.1 Undifferenced Multi-GNSS PPP Model

PPP utilizes precise products obtained from a global network to eliminate satellite orbit and clock error. Also, the ionosphere-free linear combination (IF) of dual-frequency code and phase observations are used in the standard PPP model to remove the first-order ionospheric effect on GNSS signals (Zumberge et al., 1997; Kouba and Héroux, 2001). As a standard, the precise products generated by IGS (International GNSS Service) has been employed by the GNSS users for eliminating satellite-induced error sources. As a part of multi-GNSS Experiment (MGEX), IGS has started to generate and distribute precise orbit and clock products for multi-constellation, i.e. GPS, GLONASS, Galileo, BeiDou and QZSS (Montenbruck et al., 2017). MGEX products generated in the same reference frame and time scale have been extensively utilized in the integration of multi-GNSS in recent years.

MGEX products are generated on the basis of the IF linear combination. Also, MGEX products, like to standard IGS products which include GPS constellation only, provides satellite clock corrections embracing code hardware biases for multi-GNSS constellations. There is not any product which contains the satellite phase hardware biases within IGS products. Satellite code hardware biases are eliminated by being assimilated into the satellite clock errors, while satellite phase hardware biases are lumped into the ambiguity parameters and estimated together with them in the PPP model. Finally, the receiver clock errors are estimated together with the receiver code hardware biases due to their high correlation (Kouba and Héroux, 2001; Steigenberger et al., 2014). Considering all these into account, the IF linear combinations of dual-frequency (i=1,2) code pseudorange (P) and carrier phase (L) observations can be written as

$$P_{IF,r}^{s,j} = \rho_r^{s,j} + c\widetilde{dt}_r^s - c\widetilde{dT}^{s,j} + T_r^{s,j} + \varepsilon(P_{IF,r}^{s,j}) \quad (1)$$

$$L_{IF,r}^{s,j} = \rho_r^{s,j} + c\widetilde{dt}_r^s - c\widetilde{dT}^{s,j} + T_r^{s,j} + \lambda_{IF}^s \widetilde{N}_{IF}^{s,j} + \varepsilon(L_{IF,r}^{s,j}) \quad (2)$$

with

$$c\widetilde{dt}_r^s = (\,cdt_r^s + b_{IF,r}^s\,),\; c\widetilde{dT}^{s,j} = (cdT^{s,j} + b_{IF}^{s,j}) \quad (3)$$

$$\widetilde{N}_{IF}^{s,j} = N_{IF}^{s,j} + (B_{IF,r}^s - b_{IF,r}^s) - (B_{IF}^{s,j} - b_{IF}^{s,j}) \quad (4)$$

where subscript r refers to the receiver while superscripts s and j indicate the GNSS index (*G: GPS, R: GLONASS, E: Galileo and C: BeiDou*) and the satellite number, respectively. Additionally, $\rho_r^{s,j}$ is the geometric range; c is the speed of light; $c\widetilde{dt}_r^s$ and $c\widetilde{dT}^{s,j}$ are the reformed receiver and satellite clock errors, respectively; $T_r^{s,j}$ is the tropospheric delay; $N_{IF}^{s,j}$ and λ_i^s are the ambiguity parameter and wavelength for the IF combination; ε is the observation noise; cdt_r^s and $cdT^{s,j}$ are the receiver and satellite clock errors; $b_{IF,r}^s$ and $b_{IF}^{s,j}$ are the receiver and satellite hardware code biases for the IF combination; $B_{IF,r}^s$ and $B_{IF}^{s,j}$ are the receiver and satellite hardware phase biases for the IF combination, respectively.

Equations (1) and (2) have different receiver clock parameters for each navigation system. Nevertheless, it is not feasible in practice because most of the GNSS receivers currently utilize the GPS system time as a reference timescale. Additionally, the satellite clock corrections in MGEX products use GPS time as a reference timescale (Steigenberger et al., 2014; Cai and Gao, 2013). As a result, the introduction of system time-difference parameters representing the time and hardware bias difference between navigation systems is the more preferred way when combining the multi-constellation. In general, the system time-difference parameters for GLONASS, Galileo, and BeiDou are introduced with respect to the GPS time (Cai and Gao, 2013; Li et al., 2015). After applying the precise products and introducing the system time-difference parameters, the IF observation equations of GPS, GLONASS, Galileo, and BeiDou can be written as

$$P_{IF,r}^{G,j} = \rho_r^{G,j} + c\widetilde{dt}_r^G + T_r^{G,j} + \varepsilon(P_{IF,r}^{G,j}) \quad (5)$$

$$L_{IF,r}^{G,j} = \rho_r^{G,j} + c\widetilde{dt}_r^G + T_r^{G,j} + \lambda_{IF}^G \widetilde{N}_{IF}^{G,j} + \varepsilon(L_{IF,r}^{G,j}) \quad (6)$$

$$P_{IF,r}^{R,j} = \rho_r^{R,j} + c\widetilde{dt}_r^G + cdt_{sys}^R + T_r^{R,j} + \varepsilon(P_{IF,r}^{R,j}) \quad (7)$$

$$L_{IF,r}^{R,j} = \rho_r^{R,j} + c\widetilde{dt}_r^G + cdt_{sys}^R + T_r^{R,j} + \lambda_{IF}^R \widetilde{N}_{IF}^{R,j} + \varepsilon(L_{IF,r}^{R,j}) \quad (8)$$

$$P_{IF,r}^{E,j} = \rho_r^{E,j} + c\widetilde{dt}_r^G + cdt_{sys}^E + T_r^{E,j} + \varepsilon(P_{IF,r}^{E,j}) \quad (9)$$

$$L_{IF,r}^{E,j} = \rho_r^{E,j} + c\widetilde{dt}_r^G + cdt_{sys}^E + T_r^{E,j} + \lambda_{IF}^E \widetilde{N}_{IF}^{E,j} + \varepsilon(L_{IF,r}^{E,j}) \quad (10)$$

$$P_{IF,r}^{C,j} = \rho_r^{C,j} + c\widetilde{dt}_r^G + cdt_{sys}^C + T_r^{C,j} + \varepsilon(P_{IF,r}^{C,j}) \quad (11)$$

$$L_{IF,r}^{C,j} = \rho_r^{C,j} + c\widetilde{dt}_r^G + cdt_{sys}^C + T_r^{C,j} + \lambda_{IF}^C \widetilde{N}_{IF}^{C,j} + \varepsilon(L_{IF,r}^{C,j}) \quad (12)$$

where cdt_{sys}^R, cdt_{sys}^E and cdt_{sys}^C indicate the system time difference parameters for GLONASS, Galileo and BeiDou with respect to GPS time, respectively. Equations (5) to (12) represent the undifferenced multi-GNSS PPP model, and its unknown parameters are three position components, one receiver clock error, three system time-difference parameters, one tropospheric delay and one real-valued ambiguity parameter for each of the observed satellites.

2.2 Processing Strategies

In this study, PPPH, an open-source GNSS analysis software, which is able to integrate multi-GNSS, is utilized to perform PPP processes (Bahadur and Nohutcu, 2018). PPPH is based on the undifferenced multi-GNSS PPP model described in the previous section. The details of processing strategies employed to mitigate PPP error sources are given in Table 1.

Table 1. Processing strategies applied for PPP solutions in the study.

Constellation	GPS, GLONASS, Galileo, BeiDou
Processing mode	Static
Satellite orbit and clock	Final GFZ products
Satellite antenna phase center offsets (PCOs) and its variations (PCVs)	IGS absolute antenna model (Antex), if not available, conventional values for Galileo and BeiDou (Rizos et al., 2013)
Receiver antenna PCOs and PCVs	IGS absolute antenna model (Antex), if not available, GPS values for Galileo and BeiDou
Troposphere Dry component Wet component Mapping function Gradients	 Modeled by Saastamoinen (1972) with Global Pressure and Temperature 2 model (Lagler et al., 2013) Estimated Global Mapping Function (Böhm et al., 2006) Not applied or estimated
Relativistic effects	Corrected (Kouba, 2015)
Phase wind-up	Corrected (Wu et al., 1993)
Site displacements effects	Solid Earth tides and ocean loading are corrected (Petit and Luzum, 2010)
Adjustment method	Extended Kalman filter
Elevation mask	8°
Weighting method for observation	Elevation dependent, correlations ignored
Standard deviations of observables	Carrier phase: 0.003 m at zenith Code pseudorange: 3 m at zenith
The standard deviation ratios between GPS, GLONASS, Galileo, and BeiDou, respectively	Carrier phase : 1 : 1 : 2 : 2, Code pseudorange: 1 : 2 : 2 : 2

3. TEST AND RESULTS

In order to investigate the usability of multi-GNSS PPP method with 1-s observation sampling rate in establishing GCPs, an experimental test was conducted. Firstly, 24-hour observation datasets collected at four MGEX stations during the 5-day period of January 7-11, 2019 were acquired from IGS FTP servers. These stations are equipped with multi-GNSS receivers which are able to record observations of GPS, GLONASS, Galileo and BeiDou constellations with 1-s observation sampling rate. Since the high-rate observations are not available for all MGEX stations, the stations located nearest Turkey as possible are selected for the test. The geographical locations of the stations employed in the test are given in Figure 1.

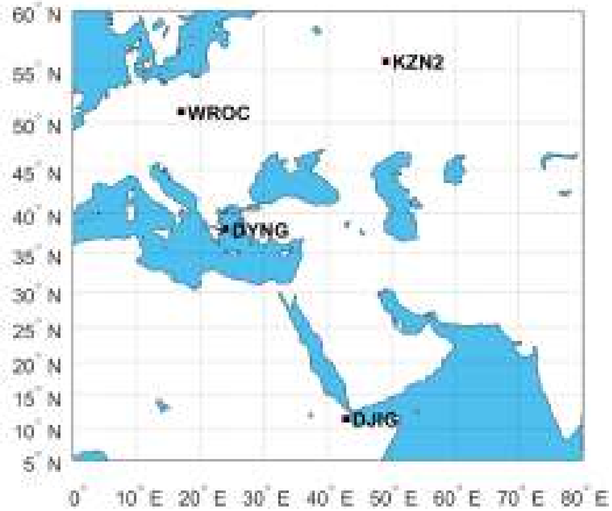

Figure 1. Geographical locations of MGEX stations used in this study.

The second observation dataset with 30-s sampling rate was obtained by decimating the original dataset. In order to investigate the PPP performance more detailed, 5-day observation datasets were divided into 2-hour periods. So, 12 periods for each day and 60 periods for the test period were obtained. Two different datasets with 1- and 30-second sampling rates were processed in PPPH software under two PPP modes, which are GPS-only and multi-GNSS containing GPS, GLONASS, Galileo and BeiDou constellations. On the other hand, the results obtained from PPP processes were evaluated in terms of positioning accuracy and convergence time. The positioning error is computed as the difference between the related PPP solution and the ground truth at the end of the related process period (2 hours). IGS weekly solutions, which include very precise station coordinates, were used as the ground truth in this study. On the other hand, the convergence time was determined as the time when a sub-decimetre 3D positioning accuracy is achieved and subsequently sustained for a period longer than 10 min.

Table 2 indicates the average positioning errors and convergence times obtained from the PPP processes of four stations over a period of 5 days under GPS-only and multi-GNSS PPP modes with 1- and 30-s observation sampling rates, separately. The positioning errors are calculated in the local coordinate system as including north, east and up directions. Also, three-dimensional (3D) positioning errors are presented in Table 2. From the table, we can see that the integration of four constellations, namely multi-GNSS, improves the PPP performance in terms of positioning accuracy and convergence time, substantially. Additionally, the increase of observation sampling rate from 30-s to 1-s enhances the positioning accuracy of PPP solutions with a limited amount, while the use of high observation sampling significantly reduces the average convergence time. Finally, we can say that the multi-GNSS PPP solution with 1-s sampling rate provides better positioning performance compared with the other PPP solutions. In multi-GNSS PPP mode with the 1-s sampling rate, the average convergence time is about 16 minutes, which is less than half of convergence time of GPS-only PPP solutions with the 30-s sampling rate.

Table 2. Averaged positioning errors and convergence time obtained from GPS-only and Multi-GNSS PPP solutions at the end of 2-hr process periods with 1 and 30-s sampling rate.

Sampling Rate (s)	**PPP Mode**	**Positioning Error (mm)**				**Convergence Time (min)**
		N	**E**	**U**	**3D**	
30	GPS-only	14.7	31.0	43.8	62.2	37.32
	Multi-GNSS	12.3	19.2	29.0	41.7	22.37
1	GPS-only	14.2	29.7	42.1	59.6	25.14
	Multi-GNSS	12.2	18.4	27.1	39.8	15.95

Figure 2 shows the temporal variations of the percentage of converged periods within the whole periods for GPS-only and multi-GNSS PPP solutions with 30- and 1-s observation sampling rates. As can be seen from the figure, the percentage of converged periods for multi-GNSS PPP solution with 1-s observation sampling rate is considerably higher than the other solutions within a short period of time. For example, the percentage of converged periods for GPS-only PPP solutions with 30-s sampling rate is under 10% at 10 minutes, while the percentage for multi-GNSS PPP solutions with 1-s sampling rate is over 40% for the same time. From the figure, we can conclude that multi-GNSS PPP solutions with the higher observation sampling rate achieve more converged periods within a short period of time, which offers a considerable opportunity for establishing GCPs.

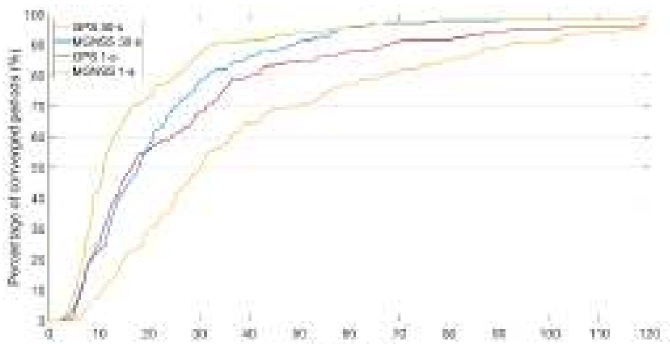

Figure 2. Variation of the percentage of converged periods within all periods with respect to time for GPS-only and multi-GNSS PPP modes on the basis of 30- and 1-s observation sampling rates.

4. SUMMARY AND CONCLUSİONS

In this study, the usability of PPP technique in establishing GCPs was investigated. For this purpose, an experimental test, which includes observation datasets collected at four IGS stations during a 5-day period of 7-11 January 2019, was performed. In the test, observation datasets were processed under GPS-only and multi-GNSS PPP modes with 30-s and 1-s observation sampling rates, separately using PPPH software. The results obtained from

PPP solutions were evaluated in terms of positioning accuracy and convergence time.

The results indicate that the integration of four GNSS constellations, namely multi-GNSS, enhances the PPP performance significantly in comparison with the traditional PPP approach containing GPS satellites only. Moreover, the increase of observation sampling rate from 30-s to 1-s improves convergence time for both GPS-only and multi-GNSS PPP modes, substantially. Multi-GNSS PPP solutions with 1-s observation sampling rate provide better positioning performance compared with the other PPP solutions in terms of positioning accuracy and convergence time. In addition, the results prove that multi-GNSS PPP solutions with the higher observation sampling rate reach considerably more converged periods within a short period of time. Nearly 95% of the whole periods were converged within 30 minutes in multi-GNSS PPP solutions with 1-s observation sampling rate. Also, the average convergence time is 16 minutes for multi-GNSS PPP solution with the 1-s sampling rate. Considering the instructions on how to establish and measure the GCPs in Turkey, the results indicate that multi-GNSS PPP solution with the 1-s observation sampling rate can be used as an alternative method for establishing GCPs.

REFERENCES

Ackermann, F., 1994. Practical experience with GPS supported aerial triangulation. *The Photogrammetric Record*, 14(84): 861–874.

Bahadur, B., Nohutcu, M., 2018. PPPH: a MATLAB-based software for multi-GNSS precise point positioning analysis. *GPS Solutions*, 22:113.

Böhm, J., Niell, A., Tregoning, P., Schuh, H., 2006. Global Mapping Function (GMF): A new empirical mapping function based on numerical weather model data. *Geophysical Research Letters*, 33.

Cai, C., Gao, Y., 2013. Modelling and assessment of combined GPS/GLONASS precise point positioning. *GPS Solutions*,17(2): 223-236.

Cai, C., Gao, Y., Pan, L., Zhu, J., 2015. Precise point positioning with quadconstellations: GPS, BeiDou, GLONASS, and Galileo. *Advances in Space Research*, 56 (1): 133–143.

Choy, S., Bisnath, S., Rizos, S., 2017. Uncovering common misconceptions in GNSS Precise Point Positioning and its future prospect. *GPS Solutions,* 21(1):13–22.

Kouba, J., Héroux, P., 2001. Precise Point Positioning Using IGS Orbit and Clock Products. *GPS Solutions* 5(2):12-28.

Kouba, J., 2015. A Guide to Using International GNSS Service (IGS) Products, https://kb.igs.org/hc/en-us/articles/201271873-A-Guide-to-Using-the-IGS-Products

Lagler, K., Schindelegger, M., Böhm, J., Krásná, H., Nilsson, T., 2013. GPT2: Empirical slant delay model for radio space geodetic techniques. *Geophysical Research Letters*, 40(6):1069-1073.

Li, X., Ge, M., Dai, X., Ren, X., Fritsche, M., Wickert, J., Schuh, H., 2015. Accuracy and reliability of multi-GNSS real-time precise positioning: GPS, GLONASS, BeiDou, and Galileo. *Journal of Geodesy,* 89(6): 607-635.

Montenbruck, O., Steigenberger, P., Prange, L., Deng, Z., Zhao, Q., Perosanz, F., Romero, I., Noll, C., Stürze, A., Weber, G., Schmid, R., MacLeod, K., Schaer, S., 2017. The Multi-GNSS Experiment (MGEX) of the International GNSS Service (IGS) – Achievements, prospects and challenges. *Advances in Space Research* 59 (7): 1671-1697.

Murtiyoso, A., Grussenmeyer, P., 2017. Documentation of heritage buildings using close-range UAV images: dense matching issues, comparison and case studies. *The Photogrammetric Record*, 32(159): 206–229.

Peppa, M.V., Mills, J.P., Moore, P., Miller, P.E. Chambers, J.E., 2016. Accuracy assessment of a UAV-based landslide monitoring system. *International Archives of Photogrammetry, Remote Sensing and Spatial Information Sciences*, 41(B5): 895–902.

Petit, G., Luzum, B., 2010. IERS Conventions 2010, IERS Technical Note 36, Frankfurt am Main: Verlag des Bundesamts für Kartographie und Geodäsie, 179 pp., ISBN 3-89888-989-6.

Rizos, C., Janssen, V., Roberts, C., Grinter, T., 2012. Precise point positioning: is the era of differential GNSS positioning drawing to an end, FIG Working Week 2012, Roma, Italy.

Rizos, C., Montenbruck, O., Weber, R., Weber, G., Neilan, R., Hugentobler, U., 2013. The IGS MGEX Experiment as a Milestone for a Comprehensive Multi-GNSS Service. In: Proceedings of the ION 2013 Pacific PNT Meeting, Honolulu, Hawaii, April 2013, 289-295.

Saastamoinen, J., 1972. Contributions to the theory of atmospheric refraction. *Bulletin Geodesique*, 105(1): 279–298.

Steigenberger, P., Hugentobler, U., Loyer, S., Perosanz, F., Prange, L., Dach, R., Uhlemann, M., Gendt, G., Montenbruck, O., 2015. Galileo orbit and clock quality of the IGS Multi-GNSS Experiment. *Advances in Space Research*, 55(1): 269-281.

Tegedor, J., Øvstedal, O., Vigen, E., 2014. Precise orbit determination and point positioning using GPS, GLONASS, Galileo and BeiDou. *Journal of Geodetic Science*, 4 (1): 65–73.

Wu, J.T., Wu, S.C., Hajj, G.A., Bertiger, W.I., Lichten, S.M., 1992, Effects of antenna orientation on GPS carrier phase, *Manuscripta Geodaetica*, 18(2): 91-98.

Xu, P., Shi, C., Fang, R., Liu, J., Niu, X., Zhang, Q., Yanagidani, T., 2013. High-rate Precise Point Positioning (PPP) to measure seismic wave motions: an experimental comparison of GPS PPP with inertial measurement units. *Journal of Geodesy*, 87(4): 361-372.

Yuan, X. X., 2009. Quality assessment for GPS-supported bundle block adjustment based on aerial digital frame imagery. *The Photogrammetric Record*, 24(126): 139–156.

Zumberge, J.F., Heflin, M.B., Jefferson, D.C., Watkins, M.M., Webb, F.H., 1997. Precise point positioning for the efficient and robust analysis of GPS data from large networks. *Journal of Geophysical Research-Solid Earth* 102(B3): 5005-5017.